https://dx.doi.org/10.22161/ijaers.6.3.5 ISSN: 2349-6495(P) | 2456-1908(O)

A Comparative Analysis of PID, Fuzzy and H Infinity Controllers Applied to a Stewart Platform

Ricardo Breganon[1], Marcio A.F. Montezuma[2], Mateus M. de Souza[3], Rodrigo C. Lemes[3], Eduardo M. Belo[4]

[1]Federal Institute of Paraná, JACAREZINHO, PARANÁ, BRAZIL
[2]Federal Technologic University of Paraná, CORNÉLIO PROCÓPIO, PARANÁ, BRAZIL
[3]Federal Institute of São Paulo, SÃO CARLOS, SÃO PAULO, BRAZIL
[4]Engineering School of São Carlos - Universityof São Paulo, SÃO CARLOS, SÃO PAULO, BRAZIL

***Abstract*—*This work presents the design of three controllers, the H infinity controller with output feedback, the PID controller and the Fuzzy controller applied to a Stewart platform. The actuator model was obtained by a step voltage input to the electric motor and measuring its displacement by the encoders coupled, in each of the respective axes of the motors. The motion transmission relation mechanism between the motor shaft and each actuator is obtained by the displacement spindle from the rotation of motor which are measured by the corresponding encoder. The kinematics and dynamics platform's data compose the whole systems models. Several experiments were carried out on the real Stewart platform with the help of an XsensMTi-G inertial sensor to measure the Platform Euler angles. The experimental results obtained by the three controllers were satisfactory in position control and orientation of the Stewart platform.*

***Keywords*—PID Controller, Fuzzy Controller, H infinity Controller, Stewart Platform**.

I. INTRODUCTION

Stewart Platforms are composed of two platforms connected by six parallel linear actuators. Extending or retracting actuators can change the relative position between the two platforms. It can be applied in flight simulators, cars simulators, machining of parts and other applications [1].

Attitude and position control of Stewart platforms are complexing problems in several areas of study [9]. They were obtained using different techniques like, PID controllers with gains obtained by cooperative co-evolution algorithm [2], fuzzy PID and feedback controllers with gains defined in reference points and selected in other points by fuzzy algorithm [1], [3], [6], PD controller with gains varying with adaptive algorithm [4], H infinity controller [5], [7].

In this work, it was used the Stewart platform designed by the Airspace Control Laboratory of the Engineering School of São Carlos – USP. The Figure 1 shows the Stewart platform utilized. It has six electromechanical actuators that are utilized to control the position and attitude of the movable platform. To measure the variation in the actuators' lengths it was used encoders in the shaft of the actuators' motors to measure the number of rotations, and then it has been applied a calibration curve to obtain the actuator length. It was used the acquisition, transmitting, and processing system dSPACE in combination with the speed controller drive RoboClaw 2 and an inertial sensor XsensMTi-G measurement of the Euler angles of the Stewart Platform [7].

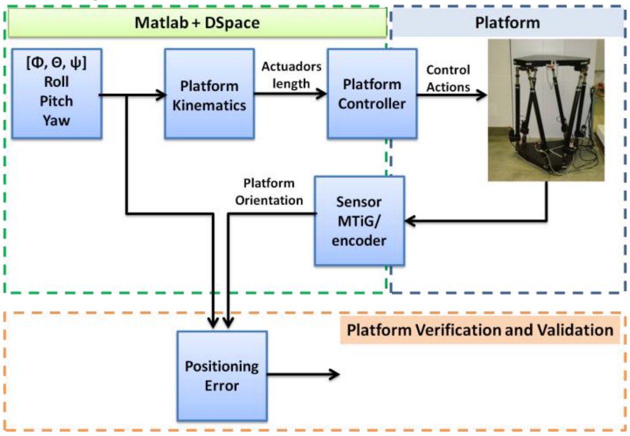

Fig. 1: Stewart platform of the Airspace Control Laboratory.

II. INVERSE KINEMATIC

Defined position and attitude of the Stewart platform, length of six actuators can be obtained using the inverse kinematic of the platform. Joints of actuators and platforms are known for a given platform, and it can be written in relation with the center of each platform in two

https://dx.doi.org/10.22161/ijaers.6.3.5 **ISSN: 2349-6495(P) | 2456-1908(O)**

coordinate systems, shown in Figure 2. The base platform coordinate system utilizes the center of the base platform F as origin, the xf-axis pointing between joints with actuators 1 and 6, zf-axis is perpendicular with the platform plane, and yf-axis completes the right-hand rule. The movable platform coordinate system center M and its axis xm, ym, and zm are defined in a similar way. The joints positions of the base and movable platforms, in its coordinate systems, are shown in Equation (1) and Equation (2), respectively.

$$\{F_i\}^F = \{F_{i1} \quad F_{i2} \quad 0\}^T, i = 1,2,\ldots,6 \qquad (1)$$

$$\{M_i\}^M = \{M_{i1} \quad M_{i2} \quad 0\}^T, i = 1,2,\ldots,6 \qquad (2)$$

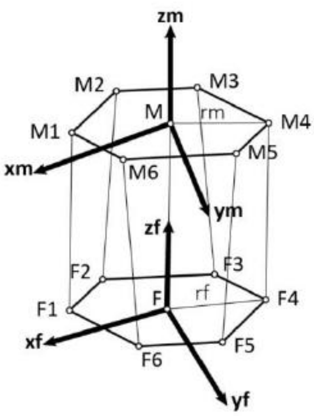

Fig. 2: Base and movable platforms coordinate systems.

The transformation matrix [T^{MF}] to obtaining coordinates of the movable coordinate system for the base coordinate system, can be obtained by using three rotations in sequence. The first rotation is applied in xm-axis until ym-axis is parallel to the base platform plane and this angle of rotation φ is known as roll angle. Then a rotation is appliedin the ym-axis until the movable platform is parallel to the base platform, so the pitch θ is obtained. To complete the coordinate systems, a last rotation is applied in the zm-axis generating the yaw angle ψ. The transformation matrix is show in Equation (3).

$$[T^{MF}] = \begin{bmatrix} c\varphi c\theta & c\,\varphi\, s\theta s\psi - s\varphi c\psi & c\,\varphi\, s\theta\, c\,\psi + s\varphi s\psi \\ s\varphi c\theta & s\varphi s\theta\, s\psi + c\,\varphi\, c\psi & s\varphi s\theta\, c\,\psi - c\,\varphi\, s\psi \\ -s\theta & c\,\theta\, s\psi & c\,\theta\, c\psi \end{bmatrix} \qquad (3)$$

where c is the cosine and s is the sine function.

The position of the movable platform can be written in the base platform system as shown in Equation (4), then length vectors V_i of six actuators can be obtained utilizing Equation(5) and shown in Figure 3.

$$\{M\}^F = \{x \quad y \quad z\}^T \qquad (4)$$

$$\{V_i\}^F = \{V_{i1} \quad V_{i2} \quad V_{i3}\}^T = \{M\} + [T^{MF}] \times \{M_i\} - \{F_i\}, \quad i = 1,2,\ldots,6 \qquad (5)$$

The actuator's length l_i is the module of the vector $\{V_i\}$ as shown in Equation (6) [8].

$$l_i = \{{V_{i1}}^2 \quad {V_{i2}}^2 \quad {V_{i3}}^2\}^{0.5}, \qquad i = 1,2,\ldots,6 \qquad (6)$$

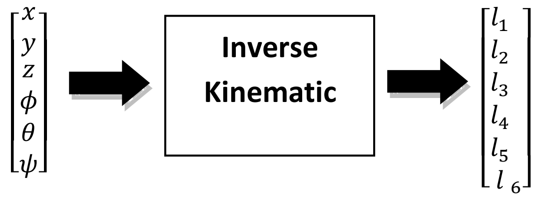

Fig. 3:Inverse Kinematic

III. PID CONTROLLER

We used the PID controller which is widely known, with transfer function presented in Equation (7). A controller was designed and this was applied to each of the six actuators independently [9]. The controller takes as input the signal from the error between the desired actuator length and actual length and then defines the control action that is the sum of proportional, derivative and integrative actions.

$$\frac{U}{E}(s) = \frac{kd(s^2 + \frac{kp}{kd}s + \frac{ki}{kd})}{s} \qquad (7)$$

IV. FUZZY CONTROLLER

The position and attitude control of the movable platform in relation to the base platform is executed by controlling the six actuators lengths. A small variation in the response of each real eletromechanical actuator is expected and can cause undesired movement of the movable base, in the case of an actuator reaches the desired length before others. To avoid this situation, a fuzzy logic controller was designed to control all the actuators with only one controller [1, 10].

The controller receives the desired position and attitude of the movable platform, utilizes the inverse kinematic to obtain desired lengths for the six actuators, and using two fuzzy sets it sends signals of voltage to the electric motor of each actuator. To define the amplitude and time of application of each signal, it uses the procedure described next.

First, the difference between the desired lengths and the actual lengths are calculated for all actuators and are the inputs of the fuzzy logic controller. These inputs are normalized utilizing the variation of the actuator´s length when applied a tension of 10V in its electric motor during 1 second. The normalized inputs are used to define the actuator that will take longer to reach the desired length. Utilizing difference of this actuator the time of application of the signal is obtained.

Fuzzy sets with different variations on the actuator length were created using experimental tests in the Stewart

https://dx.doi.org/10.22161/ijaers.6.3.5 ISSN: 2349-6495(P) | 2456-1908(O)

platform. In these tests, square signals with 10V and -10V were sent to the electric motors of the actuators with different times of application and the variations in the actuator's lengths were measured. These values are presented in Table 1 and Table 2. Utilizing the triangular membership presented in Equation (7), the application time of the square signal is obtained using Equation (8).

Table.1: Variations in actuators' lengths with different time of application and amplitude of 10V [mm].

Time (s)	Act1 10V	Act2 10V	Act3 10V	Act4 10V	Act5 10V	Act6 10V
0.1	3.86	4.36	3.89	3.93	4.34	3.79
1.0	45.9	54.01	45.54	47.56	51.34	44.71
2.0	91.17	99.48	94.87	96.28	101.25	91.37
2.5	114.51	124.31	118.9	120.2	128.1	115.1

Table 2.Variations in actuators' lengths with different time of application and amplitude of -10V [mm].

Time (s)	Act1 -10V	Act2 -10V	Act3 -10V	Act4 -10V	Act5 -10V	Act6 -10V
0.1	-4.08	-3.85	-3.92	-3.83	-4.29	-4.42
1.0	-49.61	-50.23	-47.44	-47.14	-49.86	-51.45
2.0	-100.7	-98	-96.2	-94.3	-102.3	-105.1
2.5	-127.3	-122.4	-120.5	-117.8	-127.6	-131.6

$$u_{ij}^{t} = \begin{cases} \max\left[\dfrac{\Delta l_{i+1,j} - \Delta l}{\Delta l_{i+1,j} - \Delta l_{i,j}}, 0\right], i = 1, j = 1,2 \\ max\left[min\left[\dfrac{\Delta l - \Delta l_{i-1,j}}{\Delta l_{i,j} - \Delta l_{i-1,j}}, \dfrac{\Delta l_{i+1,j} - \Delta l}{\Delta l_{i+1,j} - \Delta l_{i,j}}\right], 0\right], i = \\ \max\left[\dfrac{\Delta l - \Delta l_{i-1,j}}{\Delta l_{i,j} - \Delta l_{i-1,j}}, 0\right], i = 4, j = 1,2 \end{cases} \quad (8)$$

where $\Delta l$is the higher input; $\Delta l_{i,j}$are the lengths in Tables 1 e 2 for the actuator with the high input in the i-th line and j-th column, and $u_{ij}^{t}$is the membership value for the fuzzy set $\Delta l_{i,j}$.

$$t = \sum_{i=1}^{4}\sum_{j=1}^{2} u_{ij}^{t} \times t_i \quad (9)$$

whereis the time of the applied signal and tiis the time in the i-th line of Tables1 e 2.

The amplitude of the signal for each actuator is obtained in a similar way. Square signals of voltage of 10 V, 5 V, -10 V, -5 V and minimum values of voltage that cause rotation of the actuator's motors with 0,1 s, 1 s, 2 s and 2,5 s of time of duration were sent and then the actuators lengths were measured. Table 3 shows variations of actuator's 1 length for each combination of voltage and time of application. The amplitude of the signal for each actuator is obtained utilizing Equation (10), where triangular membership functions are utilized to correlate the required variation in the length of the actuator with the amplitude voltage the controller will send to the actuator's engine.

$$V_K = \sum_{i=1}^{6} u_i^{V} \times V_i \quad (10)$$

Table 3. Variation in the actuator's 1 length [mm]

Time (s)	2.3 V	5 V	10 V	-1,3 V	-5 V	-10 V
0.1	0.05	41.82	114.52	-0.06	-52.14	-126.38
1	0.21	34.32	91.18	-0.18	-41.87	-100.74
2	0.41	17.36	45.91	-0.40	-20.64	-49.62
2.5	0.46	1.36	3.86	-0.51	-1.80	-4.09

where V_K is the amplitude of voltage of the square signal for the k-th actuator, μVi is the membership value of the desired variation in the length of the actuator obtained for the time of application of the signal and the voltage in the i-th column and Vi is the voltage in the i-th column. After the application of the square signal, this procedure is calculated again to correct for errors between the desired length and the actual length.

V. H INFINITY CONTROLLER

In the H infinity design in general weighting functions are employed to specify the stability and performance of the system. Understanding the effects of these functions on the control system is crucial for modeling specifications. A typical model for design, called augmented plant is shown in Figure 4. The weighting functions W_1, W_2 and W_3 reflect the value specified error for the regime, limitations of the control signal and the stability condition, respectively. The standard method H infinity output feedback is used to stabilize the system. The standard H infinity control problem is formulated in terms of finding a controller *K*, if one exists, such that for a given γ > 0.

$$\|T_{zw}\|_{\infty} = \left\| \begin{matrix} W_1 S \\ W_2 KS \\ W_3 T \end{matrix} \right\|_{\infty} \quad (11)$$

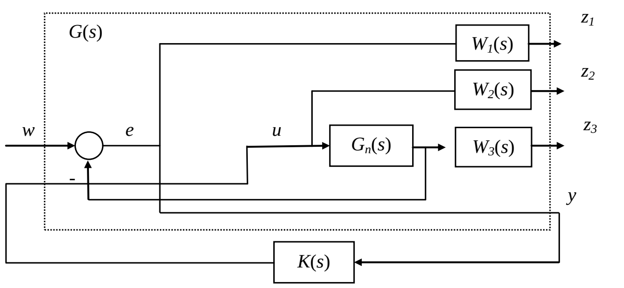

Fig.4: Augmented plant

The weighting functions represent the design specifications and modeling errors, restricting Z_1, Z_2 and Z_3 of augmented plant output, as shown below:

The $W_1(s)$ function is a limiting factor for the sensitivity function S, and should reflect the rejection of external disturbances, considering the error signal Z_1 system and tolerance to variations in the plant. The sensitivity S should take low value, especially at low frequencies. Therefore, W_1 function, which reflects the performance specifications, must submit a high value at low frequencies.

The $W_2(s)$ function weighs Z_2 that is the control signal, and must have sufficient gain capacity to limit the input control an acceptable range, avoiding the saturation of the actuator. However, a high gain can deteriorate the performance, and this commitment must be taken into account. The W_2 function is linked to limitations in the input signal of the plant G_n such as maximum voltages or currents supported by the plant.

The $W_3(s)$ function weighs Z3 namely the plant output G_n, and should minimize the peak of the complementary sensitivity function T system, reducing the oscillations and ensuring stability [11].

Thus we have the same sensitivity function$S = (I + GK)^{-1}$, the complementary sensitivity function $T = I - S$ and the sensitivity function of the controller $C = KS$.

The H infinity control in this section is based on a compensator project and an observer whose solutions are obtained by two algebraic Riccati equations and results in a controller with the same number of states of the plant [12]. P(s) is the state-space realization of an augmented plant, according to equation:

$$P(s) = \begin{bmatrix} A & B_1 & B_2 \\ C_1 & D_{11} & D_{12} \\ C_2 & D_{21} & D_{22} \end{bmatrix} \qquad (12)$$

Consider the state space representation of the augmented system, including the dynamics of the weighting functions, is given by:

$$\begin{bmatrix} \dot{x} \\ z \\ y \end{bmatrix} = \begin{bmatrix} A & B_1 & B_2 \\ C_1 & 0 & D_{12} \\ C_2 & D_{21} & 0 \end{bmatrix} \begin{bmatrix} x \\ w \\ u \end{bmatrix} \qquad (13)$$

The following hypotheses are considered in H infinity problems [12]:

(A, B_2, C_2) is stabilizable and detectable;

$D_{12}\ e\ D_{21}$ have (post) complete;

$\begin{bmatrix} A - j\omega I & B_2 \\ C_1 & D_{12} \end{bmatrix}$ has complete column post for all ω;

$\begin{bmatrix} A - j\omega I & B_1 \\ C_2 & D_{21} \end{bmatrix}$ has complete line post for all ω;

$D_{11} = 0\ e\ D_{22} = 0$;

$D_{12} = \begin{bmatrix} 0 \\ I \end{bmatrix}\ e\ D_{21} = [0 \quad I]$;

$D_{12}^T C_1 = 0\ e\ B_1 D_{21}^T = 0$ and

(A, B_1) is stabilizable and (A, C_1) is detectable.

The following Riccati equations are associated with the H infinity problem:

$$A^T X + XA + C_1^T C_1 + X(\gamma^{-2} B_1 B_1^T - B_2 B_2^T)X = 0 \qquad (14)$$

so that $Re\lambda_i[A + (\gamma^{-2} B_1 B_1^T - B_2 B_2^T)X] < 0, \forall i$ and

$$YA^T + AY + B_1 B_1^T + Y(\gamma^{-2} C_1^T C_1 - C_2^T C_2)Y = 0 \qquad (15)$$

so that $Re\lambda_i[A + Y(\gamma^{-2} C_1^T C_1 - C_2^T C_2)] < 0, \forall i$.

Given the hypotheses outlined previously, the equations of Ricatti admit stabilizing solutions $X\infty$ and $Y\infty$, and $\rho(X\infty\, Y\infty) < \gamma^2$, with $\rho(\cdot)$ the spectral radius, then there is a controller that internally stabilizes system $u = Ky$ so that the norm of the transfer function of closed loop $T_{zw} = P_{11} + P_{12}K(I - P_{22}K)^{-1}P_{21}$ is small, this is $\|T_{zw}\| < \gamma$, with γ a scalar positive [13]. The controller is given by:

$$\begin{bmatrix} \dot{x}_C \\ u \end{bmatrix} = \begin{bmatrix} A_C & B_C \\ C_C & 0 \end{bmatrix} \begin{bmatrix} x_C \\ y \end{bmatrix} \qquad (16)$$

and

$$A_C = A + \gamma^{-2} B_1 B_1^T X_\infty + B_2 F_\infty + Z_\infty L_\infty C_2 \qquad (17)$$

$$B_C = -Z_\infty L_\infty \qquad (18)$$

$$C_C = F_\infty = -B_2^T X_\infty \qquad (19)$$

$$L_\infty = -Y_\infty C_2^T \qquad (20)$$

$$Z_\infty = (I - \gamma^{-2} X_\infty Y_\infty)^{-1} \qquad (21)$$

VI. RESULT EXPERIMENTAL

To validate the controllers, a step input of 15º inψ, representing the yaw movement of the experimental Stewart Platform, the angles [ϕ θ] remained at zero. The Figures 5, 6 and 7 show the responses of the actuators to the desired input condition.

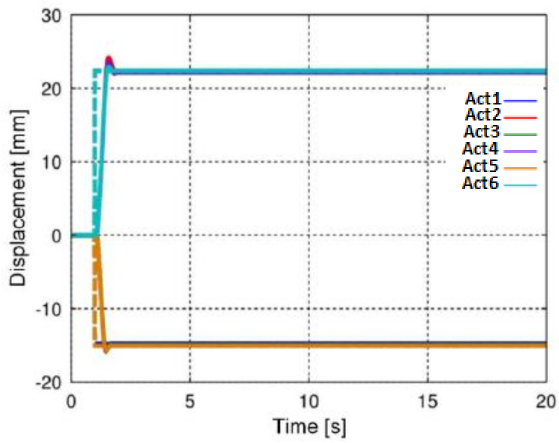

Fig.5: Response for 15º in ψ for H infinity control

https://dx.doi.org/10.22161/ijaers.6.3.5 *ISSN: 2349-6495(P) | 2456-1908(O)*

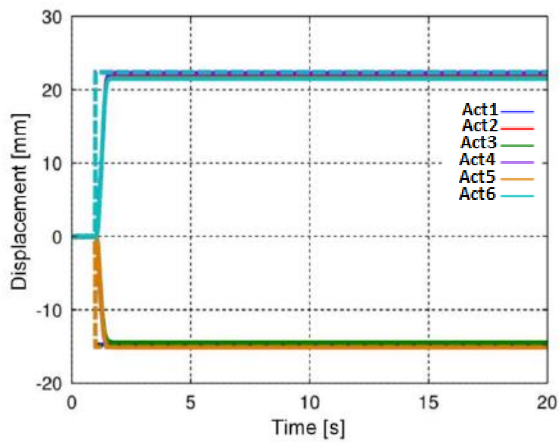

Fig. 6: Response for 15º in ψ for PID control

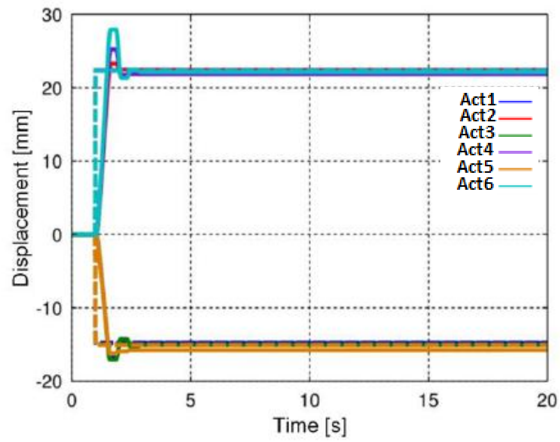

Fig.7: Response for 15º in ψ for Fuzzy control

The Figures 8, 9 and 10 show the control actions of the system to cause the actuators to reach the desired lengths. Figures 11, 12 and 13 show the error tending to zero, showing the efficiency of the designed controllers.

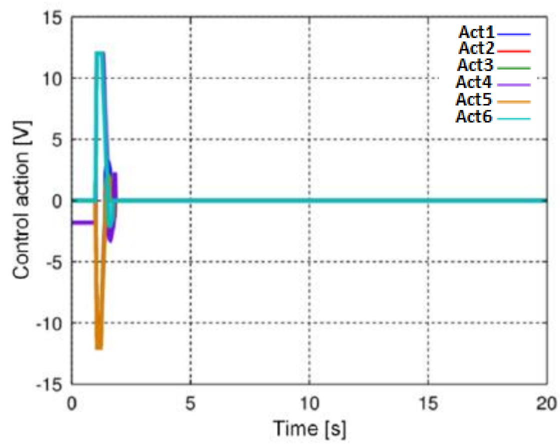

Fig.8: Control Action for 15º in ψ for H infinity control

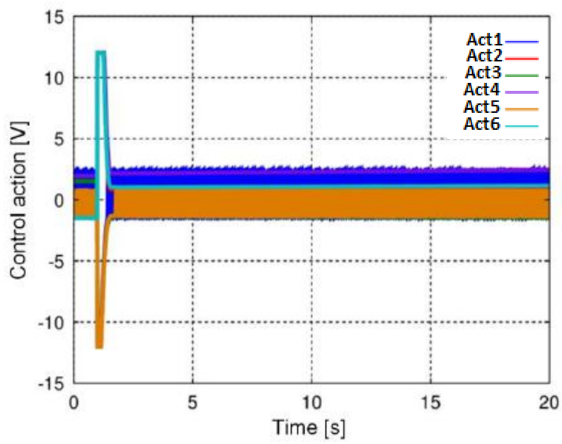

Fig. 9: Control Action for 15º in ψ for PID control

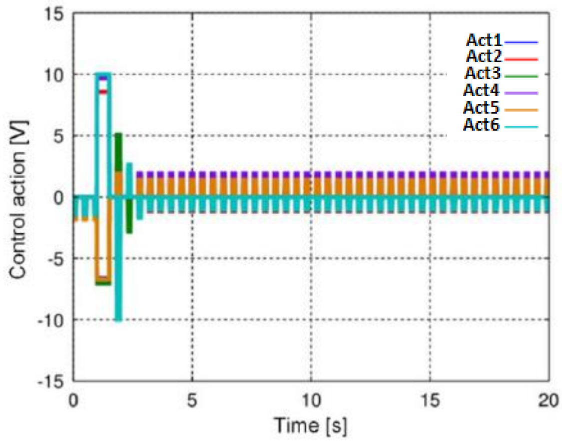

Fig. 10: Control Action for 15º in ψ for Fuzzy control

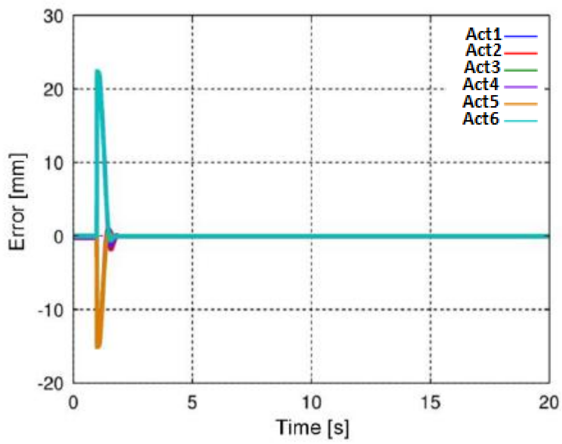

Fig. 11: Error for 15º in ψ for H infinity control

https://dx.doi.org/10.22161/ijaers.6.3.5 ISSN: 2349-6495(P) | 2456-1908(O)

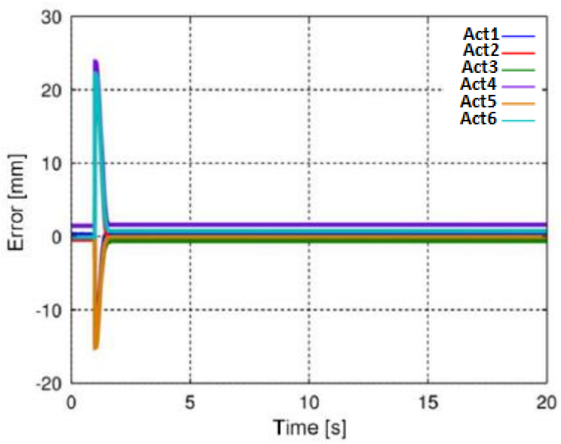

Fig.12: Error for 15º in ψ for PID control

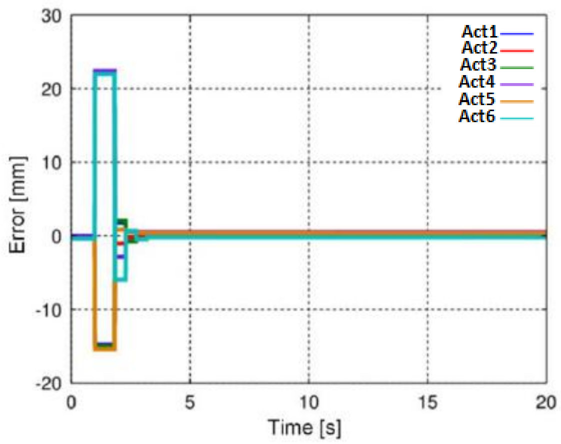

Fig.13: Error for 15º in ψ for Fuzzy control

The Figure 14 shows the orientation reading ψ for the step input of 15º, representing the yaw movement of the Stewart Platform, this acquisition is performed with the XsensMTi-G inertial sensor. It is possible to observe that, also for the movements of yaw, the controllers managed to converge to the desired orientation, but presented a regime error for this angle, where, it is necessary to say that the sensor has an accuracy of ± 1º. The Figure 15 shows the reading of the angle θ remaining close to zero degree, and the Figure 16 shows the reading of the angle φ, also close to zero degree.

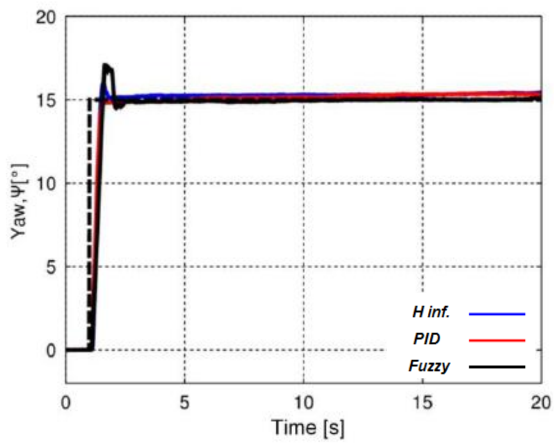

Fig.14: Yaw for ψ in 15º

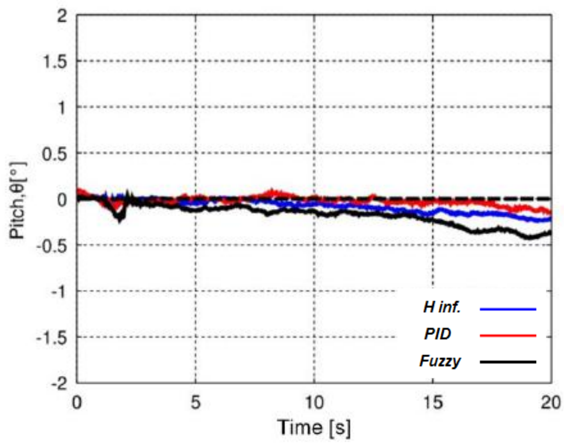

Fig 15: Pitch for ψ in 15º

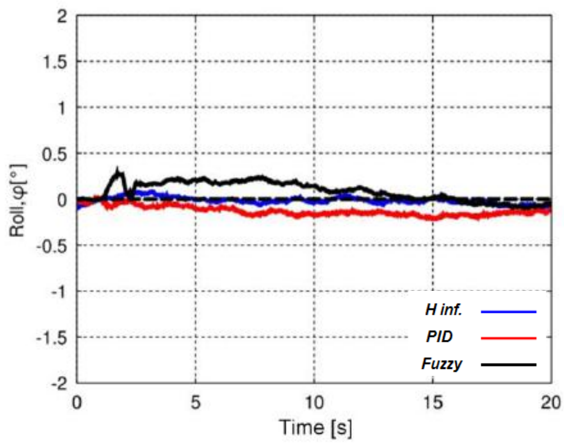

Fig 16: Roll for ψ in 15º

The angular velocities for yaw in 15° are shown in the Figures 17, 18 and 19. It is possible to observe an angular velocity peak in yaw at the beginning of the 15° step input, and as soon as the system arrives at the desired position and orientation, the velocity goes to zero.

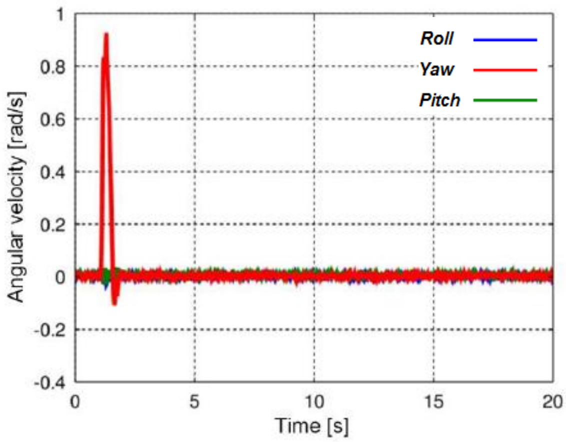

Fig. 17: Angular velocity for 15º in ψ for H infinity control

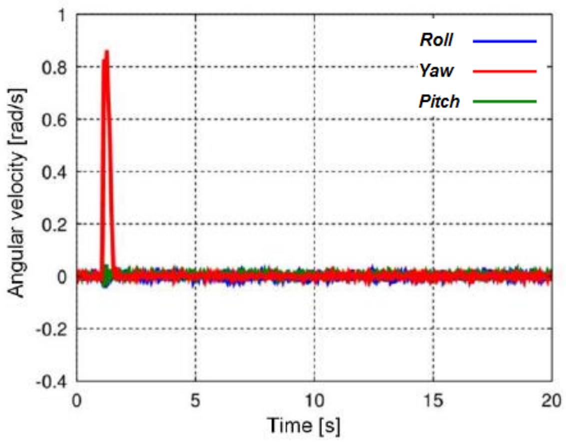

Fig. 18: Angular velocity for 15º in ψ for PID control

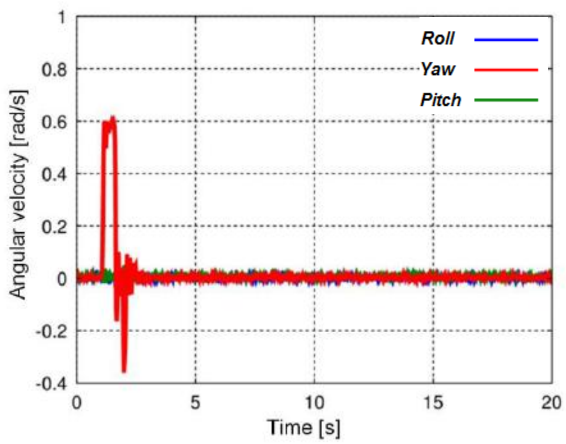

Fig. 19: Angular velocity for 15º in ψ for Fuzzy control

VII. CONCLUSION

The three controllers presented were able to efficiently control the real system of the Stewart platform, for yaw at 15º, but the H infinity controller presented the lowest regime error, as shown in Figure 11. It is also possible to observe from Figure 8 that the control action of the H infinity controller tends to zero, so the platform arrives at its desired position and orientation, presenting a greater energy savings compared to the Fuzzy and PID controllers.

ACKNOWLEDGEMENTS

This work was supported by CNPq (National Council for Scientific and Technological Development).

REFERENCES

[1] Bo, Y., Zhongcai, P. and Zhiyong, T., (2011). “Fuzzy PID control of Stewart Platform”. In *Proceedings of 2011 International Conference on Fluid Power and Mechatronics*. Beijing, China.

[2] Sun, J., Ding, Y. and Hao, K., (2008). “A cooperative co-evolutionary control method for Stewart Platform”. In *Proceedings of 2008 3rd International Conference on Intelligent System and knowledge Engineering*. Xiamen, China.

[3] Rémillard, V., Boukas, El-K., (2006) “Gough-Stewart Platform Control: A fuzzy control approach”. In *Annual Conference of the North American Fuzzy Information Processing Society*. Montreal, Canada.

[4] Nguyen, C.C., Antrazi, S.S., Zhou, Z. and Campbell, C.E. Jr., (1993). “Adaptive control of a Stewart Platform-based manipulator”. Journal of Robotic Systems, Vol. 10, p. 657-687.

[5] Ricardo Breganon, Marcio A. F. Montezuma, Mateus M. de Souza, Rodrigo C. Lemes, E. M. Belo(2018).Optimal H Infinity Controller Applied to a Stewart Platform. *International Journal of Advanced Engineering Research and Science (ISSN: 2349-6495(P)-2456-1908(O))*,5(7),051-059. http://dx.doi.org/10.22161/ijaers.5.7.7.

[6] Souza, M.M. ; Breganon, Ricardo ; Salvi, F.T.B. ; Lemes, R. C. ; Carlos, S. R. ; Moreira, E. E. T. ; Schwening, G. S. ; Belo, Eduardo Morgado (2013). A Fuzzy Technique to Control Attitude and Position of a Stewart Platform. *In: 22nd International Congress of Mechanical Engineering*, Ribeirão Preto. COBEM.

[7] Breganon, Ricardo. (2014). "Analysis, Development and Control of a Platform of Movements with 6 Degrees of Freedom" Thesis, School of Engineering of São Carlos, University of São Paulo, São Carlos.

[8] Ribeiro, S. S.(2007). Parallel Manipulators - Stewart Platform. PUC, Rio de Janeiro.

[9] Moretti, Mariana (2010).Dynamic study and simulation of a Stewart platform with emphasis on the implementation of the control. 121 p. Dissertation (Master degree in Mechanical Engineering), State University of Campinas, Faculty of Mechanical Engineering, Campinas, 2010.

https://dx.doi.org/10.22161/ijaers.6.3.5 *ISSN: 2349-6495(P) | 2456-1908(O)*

[10] Simões, M.G.; Shaw, I.S.(2007) Fuzzy Control and Modeling, 2ª Ed. São Paulo, Blucher: FAPESP, 2007.
[11] Oliveira, V.A.; Aguiar, M.L.; Vargas, J.B. (2005) Control Systems - Laboratory Classes. Department of Electrical Engineering. EESC/USP, São Carlos, SP.
[12] Doyle, J. C. et al (1989). State-space solutions to standard H2 and H∞ control problems, IEEE Transactions on Automatic Control 34(8):831–847 p.
[13] Zhou, K; Doyle, J.C and Glover, K. (1995) Robust and Optimal Control, Upper Saddle River: Prentice Hall, 1995.